THE JOURNAL OF PHYSICAL CHEMISTRY A
A JOURNAL OF THE AMERICAN CHEMICAL SOCIETY

pubs.acs.org/JPCA
Article

Insights into Ultrafast Relaxation Dynamics of Electronically Excited Furfural and 5-Methylfurfural

Wenping Wu, Baihui Feng, Yuhuan Tian, Zhigang He, Dongyuan Yang,* Guorong Wu,* and Xueming Yang

Cite This: https://doi.org/10.1021/acs.jpca.4c04503
Read Online

ABSTRACT: The ultrafast relaxation dynamics of furfural and 5-methylfurfural following excitation in the ultraviolet range is investigated using the femtosecond time-resolved photoelectron spectroscopy method. Specifically, the pump wavelength-dependent decay dynamics of electronically excited furfural and 5-methylfurfural is discussed on the basis of a detailed analysis of our measured time-resolved photoelectron spectroscopy spectra. Irradiation at all pump wavelengths prepares both furfural and 5-methylfurfural molecules with different vibrational levels in the first optically bright S_2 ($^1\pi\pi^*$) state, the lifetime of which is measured to be at least hundreds of femtoseconds. Besides the prominent deactivation channels of ring-opening and ring-puckering pathways for the $S_2(^1\pi\pi^*)$ state, we propose that there is a minor decay channel of internal conversion from the initially prepared $S_2(^1\pi\pi^*)$ state to the $S_1(^1n\pi^*)$ state. The wavepacket decays out of the Franck−Condon region on the $S_2(^1\pi\pi^*)$ state potential energy surface and bifurcates into different parts somewhere. A small fraction of the wavepacket funnels down to the $S_1(^1n\pi^*)$ state via internal conversion. The subsequently populated $S_1(^1n\pi^*)$ state contains large vibrational excess energy and decays over a lifetime of 2.5−2.8 ps. One of the deactivation channels of the $S_1(^1n\pi^*)$ state is intersystem crossing to the $^3\pi\pi^*$ triplet state. In addition, methyl substitution effects on the excited-state dynamics of furfural are also discussed. This experimental study provides new insights into the excitation energy-dependent decay dynamics of photoexcited furfural and 5-methylfurfural.

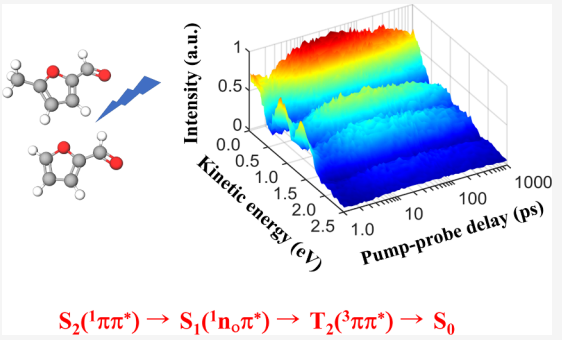

1. INTRODUCTION

Investigation of the intrinsic photochemical and photophysical behaviors of isolated small heterocyclic molecules is a prerequisite for further understanding the complicated photo-induced processes of large biomolecular systems.[1,2] Among simple five-membered heterocyclic molecules, furan is regarded as one of the prototypical molecules and the excited-state dynamics of it has been the subject of intensive experimental and theoretical studies[3−10] over the past few decades. Femtosecond time-resolved photoelectron spectroscopy (fs-TRPES) is a very powerful method to study excited-state dynamic of gas-phase heterocyclic molecules. The ultrafast nonadiabatic dynamics of furan excited in the $^1B_2(\pi\pi^*)$ state is better understood by a recent TRPES study using extreme ultraviolet probe pulses with a time resolution of 15 fs.[11] Briefly, it was suggested that ultrafast internal conversion via a ring-puckering conical intersection (CI) and a ring-opening CI takes place as predicted by computational studies.[9,10,12] The initially prepared wavepacket evolves in ∼50 fs when reaching the CIs for both ring-puckering and ring-opening pathways.[11]

In recent years, some previous studies have focused on the photochemical properties of some substituted derivatives of furan.[8,12−17] Specifically, furfural (other names, e.g., 2-furaldehyde or furan-2-carbaldehyde) is one of the aldehyde derivatives of furan. There have been two previous time-resolve studies on gas-phase isolated furfural molecule.[12,17] Oesterling et al. focused on substituent effects on the relaxation dynamics of furan, furfural and β-furfural.[12] Two time constants of 1.58 ± 0.2 ps and 140 ± 30 fs were derived from the analysis of the TRPES data of furfural upon excitation at 267 nm and ionization at 400 nm. Both time constants were assigned to the relaxation of the energetically lowest lying $\pi\pi^*$ state, while the former 1.58 ± 0.2 ps was associated with the puckering and the opening decay and the latter 140 ± 30 fs was ascribed to an additional pathway via the $n_O\pi^*$ state. They stated that their quantum chemical calculations also supported the above assignment that the shorter lifetime belongs to a deactivation via the $n_O\pi^*$ state, which is related to the aldehyde group and

Received: July 5, 2024
Revised: September 24, 2024
Accepted: September 25, 2024

thus not available in furan. It seems that a plausible picture of the deactivation mechanism of furfural at ~266 nm excitation wavelength has been proposed. However, later on, Bhattacherjee et al. employed femtosecond X-ray transient absorption spectroscopy at the carbon K-edge (~284 eV) to identify the ring-opened photoproduct generated by the photoexcitation of furfural.[17] They found that ultrafast ring opening via C−O bond fission occurs within ~350 fs in 266 nm photoexcited furfural, as evidenced by fingerprint core (carbon 1s) electronic transitions into a nonbonding orbital of the open-chain carbene intermediate at 283.3 eV.

We note that the comparison of the different time constants derived from these two time-resolved studies[12,17] was still lack of a detailed and reasonable discussion or interpretation. We are motivated by this and endeavor to achieve a more comprehensive picture of the deactivation mechanism of furfural. In this paper, we report a direct time-resolved study on the ultrafast decay dynamics of electronically excited furfural and 5-methylfurfural by using the fs-TRPES method. We focus more on the relaxation dynamics of furfural upon photoexcitation in the ultraviolet range of 238.4−267.1 nm. Irradiation at these pump wavelengths prepares furfural molecules with different vibrational levels in the first optically bright $^1\pi\pi^*$ state (S_2 at the Franck−Condon geometry, hereafter termed $S_2(^1\pi\pi^*)$). The pump wavelength-dependent photodynamics of furfural is revealed by our measured TRPES spectra. Moreover, methyl substitution effects on the excited-state dynamics of furfural are also discussed for the first time based on a comparison of the excited-state lifetimes in furfural and 5-methylfurfural.

The structures of furan, furfural and 5-methylfurfural are presented schematically in Figure 1. It has been known that

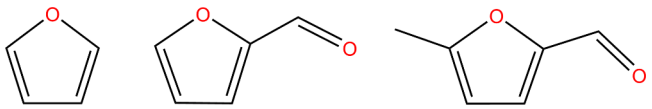

Figure 1. Furan, furfural, and 5-methylfurfural.

furfural can display two different conformations in the ground state, named the *trans* and *cis* conformers.[14] The *trans* structure of furfural is the most stable conformer in the gas phase and the relative conformation populations are *trans* (79.5%) and *cis* (20.5%) (see ref 14, ref 15, and references therein). Here we assume that the *trans* configuration of furfural is in the majority under our supersonic jet-cooled molecular beam conditions. The conformer-specific excited-state dynamics is out of the scope of the current study.

2. EXPERIMENTAL METHODS

The fs-TRPES measurements were performed on a velocity map imaging (VMI) spectrometer[18] and the experimental methods have been described in detail elsewhere.[19−22] Herein, only some key features are given. Briefly, both samples with a stated purity of ≥99.5% for furfural and ≥98% for 5-methylfurfural were purchased commercially from Macklin and used without further purification. The vapor of the liquid sample was mixed with 3 bar of helium carrier gas and expanded supersonically into a high vacuum source chamber via a 1 kHz Even-Lavie valve. The sample was heated with a valve temperature of ~45 °C throughout the experiment. The seeded molecular beam entered into the interaction chamber of the VMI spectrometer through a 1 mm skimmer. The pump wavelengths were in a range of 238.4−279.3 nm (0.1−0.4 μJ per pulse, 264−374 cm^{-1} bandwidth at full width at half-maximum (fwhm)) and the probe wavelength was chosen at 403.7 nm (3.2−4.8 μJ per pulse, 217 cm^{-1}). All laser pulses were genrated from our 1 kHz femtosecond laser system consisting primarily of a fully integrated Ti:sapphire oscillator-regenerative amplifier and two commercial optical parametric amplifiers.[23] The pump and probe laser pulses were combined collinearly on a dichroic mirror without further compression, and then focused using a CaF_2 lens (typically f/75 for the pump and f/60 for the probe laser beam) into the interaction region of the VMI spectrometer to intersect the molecular beam. All pump and probe pulses were linearly polarized and the polarization direction was parallel to the microchannel plate (MCP)/phosphor screen detector. The pump−probe time delays were scanned back and forth hundreds of times to minimize the effects caused by the fluctuations and drifts in the laser pulse energies, pointing, molecular beam intensity, etc. The two-color nonresonant ionization of NO molecules served to measure the time-zero and the cross-correlation (i.e., instrumental response function (IRF)) of the experiments. The [1 + 2′] IRFs were experimentally measured to be 120 ± 10 fs (fwhm) based on the approximation that both pump and probe laser pulses were a Gaussian profile.

3. RESULTS AND DISCUSSION

In the present work, a femtosecond laser pulse of 403.7 nm was chosen as the probe laser for two-photon ionization, while the pump laser wavelength was tunable in the ultraviolet range. At pump wavelengths of 267.1, 251.2, and 238.4 nm, the [1 + 2′] TRPES spectra of furfural are shown in Figure 2a,b,c. Note that a combination of linear (≤1 ps) and logarithmic (≥1 ps) scales is used in the time delay coordinate. The main feature of these spectra shows an extremely fast decay dynamics on a time scale of subpicosecond, followed by a much weaker and slower decay dynamics. At 251.2 and 238.4 nm, the pump−probe photoelectron signal shows a delayed rise with a maximum of about 10 ps. This feature is more pronounced and can be easily recognized by visual inspection at 238.4 nm if a portion (at delays of >1 ps) of the TRPES spectrum is scaled by a factor of 20. As shown in Figure 2a,b,c, the photoelectron kinetic energy distributions are broad and diffuse at all delays. The energetic limit for two-color [1 + 2′] ionization to the ground state (D_0) of the furfural cation is indicated by the dotted white line (labeled as 1 + 2′ cutoff). Here the value of the energetic limit is calculated using an adiabatic ionization potential of 9.22 eV[14,24] and the central pump and probe photon energies. The structure of the whole photoelectron spectra can be explained by the high-resolution He(I) photoelectron spectrum of furfural.[14] For example, as shown in Figure 2a, the [1 + 2′] TRPES spectrum of furfural upon excitation at 267.1 nm displays three broad bands, two of which are peaking at about 0.7 and 1.3 eV and assigned to two-color [1 + 2′] ionization to the ground state, $D_0(\pi^{-1})$ and the first excited state, $D_1(n_O^{-1})$ of the furfural cation. The other band below 0.4 eV is most likely to be associated with [1 + 2′] ionization of the second excited state, $D_2(\pi^{-1})$ of the furfural cation. As the pump wavelength decreases from 267.1 to 238.4 nm, the overall structures and positions of these three bands do not shift to higher kinetic energies. This strongly indicates that a series of Rydberg states are involved in the probe process.[15]

https://doi.org/10.1021/acs.jpca.4c04503
J. Phys. Chem. A XXXX, XXX, XXX−XXX

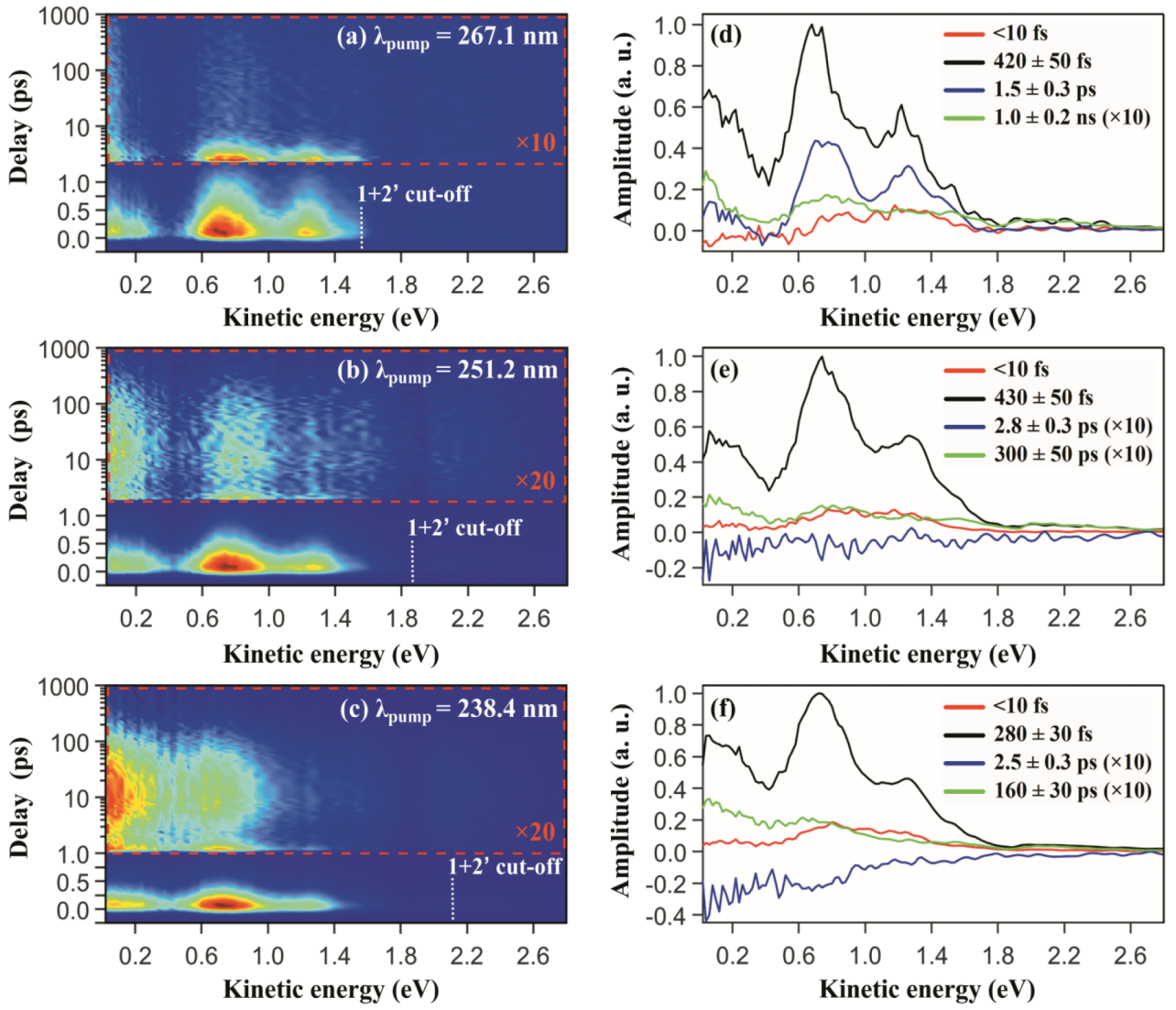

Figure 2. (a) TRPES spectrum of furfural upon excitation at 267.1 nm and ionization at 403.7 nm. A portion of it is scaled by a specific factor for better presentation. The background photoelectrons generated from single-color multiphoton ionization have been subtracted. Note that a combination of linear (≤1 ps) and logarithmic (≥1 ps) scales is used in the ordinate. The dotted white line denotes the predicted maximum photoelectron kinetic energy cutoff for [1 + 2′] ionization based on the $D_0(\pi^{-1})$ adiabatic ionization potential of furfural and the central pump and probe photon energies. (b, c) Same as (a), but at pump wavelengths of 251.2 and 238.4 nm, respectively. (d–f) Decay associated spectra (DAS) derived from the 2D global least-squares fit to the corresponding TRPES data shown in (a–c).

In order to extract more detailed dynamics information, such as time constants and decay associated spectra (DAS), a 2D global least-squares method was employed to simultaneously fit the TRPES data at all time delays and photoelectron kinetic energies. The excited-state decay process can be described using muti-exponential decay function as the following expression:

$$\text{for } t \geq 0,\ I(t, \varepsilon_k) = \sum_{i=1}^{n} \mathrm{DAS}_i(\varepsilon_k) \times \exp(-\frac{t}{\tau_i})$$
$$\text{for } t < 0,\ I(t, \varepsilon_k) = 0 \quad (1)$$

Herein, t is the time delay and ε_k is the kinetic energy of the emitted photoelectron. $\mathrm{DAS}_i(\varepsilon_k)$ represents the amplitude of the decay associated spectrum associated with time constant, τ_i. The experimentally observed pump–probe signal, $S(t)$, should be a convolution of a Gaussian cross-correlation function (i.e., IRF) and the exponential decay of excited state population, $I(t)$. As a consequence, the corresponding simulated 2D TRPES spectrum can be expressed as the following equation:

$$S(t, \varepsilon_k) = \sum_{i=1}^{n} \mathrm{DAS}_i(\varepsilon_k) \times \{[\exp(-\frac{t}{\tau_i}) \times H(t)] \otimes \mathrm{IRF}\} \quad (2)$$

Herein, $H(t)$ is the unit step function. It should be mentioned that we use a numerical convolution approach[22] which can describes the relative detection efficiency of the excited state for a specific lifetime (τ_i) and a given fwhm value of the IRF.[25] It should be pointed out that a delayed rise of the time delay-dependent signal corresponds to a sequential kinetic process,[23] which should be revealed by the result that the amplitude of one of the decay associated spectra is negative (i.e., $\mathrm{DAS}(\varepsilon_k) < 0$).

Four different time constants (τ_1, τ_2, τ_3, and τ_4) are needed in the aforementioned equation to achieve an overall

https://doi.org/10.1021/acs.jpca.4c04503
J. Phys. Chem. A XXXX, XXX, XXX−XXX

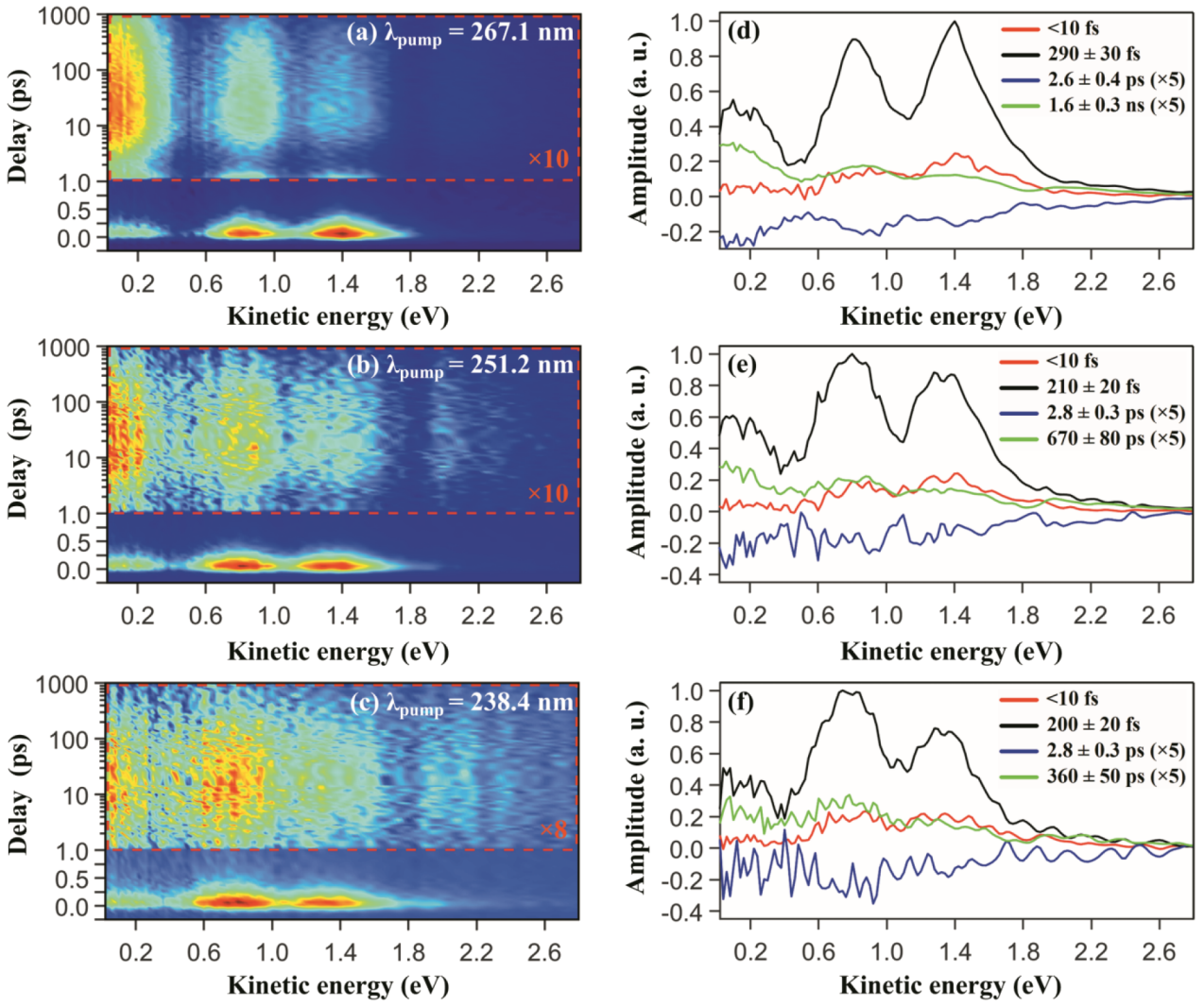

Figure 3. (a) TRPES spectrum of 5-methylfurfural upon excitation at 267.1 nm and ionization at 403.7 nm. A portion of it is scaled by a specific factor for better presentation. The background photoelectrons generated from single-color multiphoton ionization have been subtracted. Note that a combination of linear (≤1 ps) and logarithmic (≥1 ps) scales is used in the ordinate. (b, c) Same as (a), but at pump wavelengths of 251.2 and 238.4 nm, respectively. (d–f) Decay associated spectra (DAS) derived from the 2D global least-squares fit to the corresponding TRPES data shown in (a–c).

satisfactory 2D global fit to the [1 + 2′] TRPES spectra of furfural at pump wavelengths of 267.1, 251.2, and 238.4 nm. The derived time constants and their decay associated spectra are shown in Figure 2d–f for pump wavelengths of 267.1, 251.2, and 238.4 nm, respectively. The uncertainty of the derived time constants is also included based on a combined consideration of the fit quality and the error bars of both the time-zero and IRF.

Moreover, the corresponding [1 + 2′] TRPES spectra of 5-methylfurfural at pump wavelengths of 267.1, 251.2, and 238.4 nm are shown in Figure 3a–c, respectively. As revealed by visual inspection, the TRPES spectra of 5-methylfurfural share large similarities with those of furfural in the overall structure of the photoelectron kinetic energy distributions and complicated multiple exponential decay dynamics. An identical analysis is performed and the fitting results are also presented in Figure 3d–f.

At all pump wavelengths for furfural and 5-methylfurfural, the value of the time constant of τ_1 is much smaller than the time resolution of the current time-resolved experiment and labeled as <10 fs in Figure 2d–f and Figure 3d–f. As mentioned above, the detection efficiency of the excited state in photoionization-based time-resolved pump–probe measurements is sensitive to the lifetime (τ_i) of the excited state[25] especially when the value of the lifetime is much smaller than the value of the IRF. For a given intensity of the pump–probe signal, the amplitudes of DAS(ε_k) vary dramatically with the value of τ_i (e.g., τ_i < 10 fs) since the detection efficiency (described by a numerical convolution here, $\left[\exp\left(-\frac{t}{\tau_i}\right) \times H(t)\right] \otimes \mathrm{IRF}$) changes. In order to avoid misleading information about the relative amplitudes of DAS$_i$(ε_k), the τ_1 component is approximately described by DAS$_1$(ε_k)×IRF when considering the amplitudes of DAS$_1$(ε_k). For other time constants, the lifetimes of τ_2 and τ_3 are hundreds of femtoseconds and several picoseconds, respectively, while the time constant of τ_4 has the largest value.

Now we discuss the excited states involved at all pump wavelengths and the assignments of the derived time constants. According to the previous high-resolution vacuum ultraviolet

https://doi.org/10.1021/acs.jpca.4c04503
J. Phys. Chem. A XXXX, XXX, XXX–XXX

spectroscopy study,[15] the experimental 0−0 band origin of the $S_2 \leftarrow S_0$ electronic transition ($\pi^* \leftarrow \pi$) was found to be at 4.627 eV[15] (268.0 nm) for furfural, while the $S_1 \leftarrow S_0$ electronic transition ($\pi^* \leftarrow n_o$) is a very weak absorption band with an identified origin at 3.321 eV[26] (~373 nm) and a maximum at 3.75 eV[27] (~330 nm). The absolute photoabsorption cross sections of the $\pi^* \leftarrow n_o$ transition are 2 orders of magnitude smaller than those of the $\pi^* \leftarrow \pi$ transition.[15] Therefore, it is straightforward to assign the subpicosecond time constants (τ_2) to the lifetime of the $S_2(^1\pi\pi^*)$ state since the decay associated spectra at all pump wavelengths indicate that the τ_2 component is the dominant decay component, which should correspond to the depopulation rate of the initially prepared excited state. The value of τ_1 is much smaller than that of τ_2, while the intensity of the τ_1 component is relatively small when compared with that of the τ_2 component. Although sometimes we could assign such time constant (τ_1) to be associated with the relaxation of the initially prepared wavepacket out of the FC region, accompanied by a distinct decrease of photoionization efficiency.[28] This change in photoionization efficiency causes that two different time constants (τ_1 and τ_2) are needed in simulation of a continues evolution of wavepacket on the $S_2(^1\pi\pi^*)$ state potential energy surface. Herein, in the case of [1 + 2′] TRPES experiment, we prefer to assign the time constant of τ_1 to be mainly associated with the resonant [1 + 1′ + 1′] multiphoton ionization process since the [1 + 1′] excitation energies correspond to a strong absorption band of furfural.[15] At all pump wavelengths, such [1 + 1′ + 1′] signal around the time-zero actually can be approximately described using the [1 + 2′] IRF,[29] in reasonable agreement with the derived time constant of τ_1 (τ_1 < 10 fs).

As mentioned above in the Introduction, two previous time-resolved studies succeeded in observing different time constants for photoexcited furfural at 266 or 267 nm pump wavelength.[12,17] Femtosecond X-ray transient absorption spectroscopy captured a sub-400 fs ring opening process, which originates on the barrierless excited state surface.[17] This time constant is consistent with the value of 400 ± 50 fs derived from our TRPES experiment at 267.1 nm and assigned to the lifetime of some $S_2(^1\pi\pi^*)$ vibrational states slightly above the S_2 state origin. The previous 267/400 nm [1 + 2′] TRPES study observed two time constants of 1.58 ± 0.2 ps and 140 ± 30 fs.[12] The former is the same as the value of 1.5 ± 0.3 ps derived from our nearly identical measurement, while the latter is approximately described using the values of τ_1 (<10 fs) and τ_2 (420 ± 50 fs). At 267.1 nm, as shown in Figure 2d, the kinetic energy distributions of the 1.5 ± 0.3 ps component (labeled as τ_3) and the τ_2 component (420 ± 50 fs) have almost identical structure. This indicates that both time constants of 1.5 ± 0.3 ps and 420 ± 50 fs belong to the lifetimes of the $S_2(^1\pi\pi^*)$ vibrational states. In cases of some isolated heterocyclic molecules, the deactivation rate of the $^1\pi\pi^*$ state slightly above its origin could be clearly vibrational state-dependent[30,31] due to the existence of low-energy (e.g., the order of magnitude of 100 cm^{-1}) barrier on the $^1\pi\pi^*$ state multidimensional potential energy surface.

At 267.1 nm, the delayed rise profile becomes unobservable in the TRPES spectrum of furfural. This is explained by the influence of the existence of the 1.5 ± 0.3 ps component. The amplitudes of its DAS are not negative. Therefore, the assignments of this1.5 ± 0.3 ps component and the τ_3 component should be different. Besides the TPRES spectrum of furfural at 267.1 nm, there is an observable delayed rise signal at large delays (>1 ps), which is associated with the derived time constants of τ_3 and τ_4. This signal is relatively weak and its intensity is at least 1 order of magnitude smaller than that of the initial decay, the τ_2 component. The maximum of this delayed rise signal is about 10 ps, followed by a further decay with a lifetime of τ_4. The time constant of τ_3 is not the lifetime of the $S_2(^1\pi\pi^*)$ state since the amplitudes of the DAS of τ_3 are almost always negative over the whole kinetic energy range.

One reasonable explanation is that the value of τ_3 (2.5−2.8 ps) is the lifetime of a subsequently populated excited state. This intermediate state should come from the deactivation of the initially photoexcited $S_2(^1\pi\pi^*)$ state and further decay to a lower lying state, the lifetime of which is the time constant of τ_4. In the case of furfural, it was theoretically found that the $S_1(^1n\pi^*)$ state crosses the $S_2(^1\pi\pi^*)$ state somewhere on the potential energy surface.[12] Therefore, the $S_2(^1\pi\pi^*) \rightarrow S_1(^1n\pi^*)$ internal conversion channel could be one of the decay pathways of the $S_2(^1\pi\pi^*)$ state. In addition, according to excited state population of the on-the-fly dynamics simulation of furfural,[12] the $S_1(^1n\pi^*)$ state was suggested to be populated within hundreds of femtoseconds, in agreement with the above assignment that the time constant of τ_2 (430−280 fs for furfural and 290−200 fs for 5-methylfurfural) belongs to the lifetime of the $S_2(^1\pi\pi^*)$ state. As a consequence, we assign the time constant of τ_3 (2.5−2.8 ps) to the lifetime of the $S_1(^1n\pi^*)$ state. The deactivation channels of the $S_1(^1n\pi^*)$ state with large vibrational excess energy are most likely to funnel down to the ground state via the S_1/S_0 conical intersection and/or rapid intersystem crossing to a close-lying triplet state. Here the vibrationally hot ground electronic state is not expected to be detectable under the current probe conditions (two-photon ionization) since the Franck−Condon overlap between the ground state and the ionic manifold is rather poor. Thus, we would like to assign the time constant of τ_4 (1.0 ns−160 ps for furfural and 1.6 ns-360 ps for 5-methylfurfural) to a lower lying triplet state, the $T_2(^3\pi\pi^*)$ state. One consideration is the general conclusion that spin−orbit coupling between the $S_1(^1n\pi^*)$ state and the $T_1(^3n\pi^*)$ state is unimportant to the first order (the El-Sayed's rules).[32] In addition, it was found that no light is emitted from the $T_2(^3\pi\pi^*)$ state, while the $T_1(^3n\pi^*)$ state phosphoresces and has a lifetime much larger than the order of magnitude of nanosecond.[27,33] Here we propose that the subsequently populated $T_2(^3\pi\pi^*)$ state with enough large vibrational excess energy funnels down to the high vibrational levels of the ground electronic state, in good agreement with the value of τ_4 and its pump wavelength dependence.

According to the amplitudes of all the DASs, the intensity of the τ_3 and τ_4 components is minor compared with that of the τ_2 component. Thus, we speculate that this specific decay path (i.e., $^1\pi\pi^* \rightarrow {}^1n\pi^* \rightarrow {}^3\pi\pi^*$) is a minor deactivation channel. For the $S_2(^1\pi\pi^*)$ state, both the ring puckering pathway toward the ground state and the ring opening pathway via the $^1\pi\sigma^*$ state are important.[12,17] For the $S_1(^1n\pi^*)$ state, the internal conversion to the S_0 state should not be neglected.[12] All these other decay channels are not monitored by the current probe laser of 403.7 nm (3.07 eV) since two-photon energy of 6.14 eV is insufficient for the photoionization of the ring-opening intermediates and the vibrationally hot ground electronic state.

https://doi.org/10.1021/acs.jpca.4c04503
J. Phys. Chem. A XXXX, XXX, XXX−XXX

Some information can be obtained by a comparison of the measured TRPES spectra of furfural and 5-methylfurfural. The $S_2(^1\pi\pi^*)$ state origin in 5-methylfurfural is approximately 0.2 eV lower than that in furfural. Although the S_2 vibronic state-specific excitation is impossible here due to the intrinsic broad spectral bandwidth of the femtosecond pump laser pulses, we still could suggest that the 0−0 band origin of the $S_2 \leftarrow S_0$ electronic transition is close to 279.3 nm since the $[1 + 2']$ TRPES spectrum of 5-methylfurfural starts to contain a contribution of the IRF component when we slightly tune the pump laser to a longer wavelength than 279.3 nm (see Figure S1 in the Supporting Information). Here we can discuss methyl substitution effects on the excited-state dynamics of furfural in detail.

(i) The ultrafast decay mechanism of the $S_2(^1\pi\pi^*)$ state in 5-methylfurfural is similar to that in furfural. The ring-opening and ring-puckering pathways are suggested to be the dominant decay channels, while internal conversion to the $S_1(^1n\pi^*)$ state via S_2/S_1 CI seems to be a minor deactivation channel. The time constant of τ_2 is assigned to the lifetime of the $S_2(^1\pi\pi^*)$ state. For furfural and 5-methylfurfural, there is a little difference in the value of τ_2. Overall, the $S_2(^1\pi\pi^*)$ state in 5-methylfurfural decays over a shorter lifetime with similar vibrational excess energy. This can be interpreted in terms of the facilitation of the decay channel(s). The initially prepared wavepacket on the $S_2(^1\pi\pi^*)$ state potential energy surface can more easily evolve along particular coordinates involving the additional vibrational modes from the methyl group.

(ii) Another finding of our direct TRPES measurements is a specific value of τ_3, which is in a range of 2.5−2.8 ps and assigned to the lifetime of the $S_1(^1n\pi^*)$ state. Within the margin of error, the value of τ_3 is not dependent on the excitation energy and the methyl group substitution. Further explanation about this is strongly expected to be proposed based on future theoretical and experimental studies.

(iii) The lifetime of the subsequently populated $T_2(^3\pi\pi^*)$ state is observed to be strongly dependent upon the initial excitation energy, which indicates that there is a barrier on the $T_2(^3\pi\pi^*)$ state potential energy surface. Thus, the lifetime of the $T_2(^3\pi\pi^*)$ state is sensitive to the vibrational excess energy. The deactivation path of the $T_2(^3\pi\pi^*)$ vibrational states is suggested to funnel down to a hot ground state. With the addition of the methyl group, the deactivation rate of the $T_2(^3\pi\pi^*)$ state decreases. One possible explanation is that methyl substitution on furfural may increase this barrier, resulting in an overall longer lifetime for the $T_2(^3\pi\pi^*)$ state with similar vibrational excess energy.

4. CONCLUSIONS

In conclusion, the ultrafast decay dynamics of the $S_2(^1\pi\pi^*)$ state in both furfural and 5-methylfurfural is investigated using the fs-TRPES method. The deactivation mechanism of photoexcited furfural and 5-methylfurfural in a broad pump wavelength range is proposed based on a detailed analysis of the TRPES spectra. The excited-state lifetime of several hundreds of femtoseconds (1.5 ± 0.3 ps for some S_2 low-energy vibrational states slightly above the S_2 origin in furfural) is suggested to be associated with the decay of the $S_2(^1\pi\pi^*)$ vibrational states. Moreover, our experimental observation of a delayed rise in the pump−probe signal indicates that there exists a sequential kinetic process, which is explained in terms of a minor decay channel of $S_2(^1\pi\pi^*) \rightarrow S_1(^1n\pi^*) \rightarrow T_2(^3\pi\pi^*)$. In particular, a bifurcation of the initially prepared vibrational wavepacket is suggested to take place somewhere on the $S_2(^1\pi\pi^*)$ state potential energy surface and then the wavepacket partly decays into the $S_1(^1n\pi^*)$ state. The subsequently populated $S_1(^1n\pi^*)$ state contains large vibrational excess energy and has a lifetime of 2.5−2.8 ps. One of the deactivation channels of the $S_1(^1n\pi^*)$ state is intersystem crossing to the $^3\pi\pi^*$ triplet state, the lifetime of which varies with the excitation energy and the methyl substitution.

Our gas-phase TRPES study on furfural and 5-methylfurfural over a broad pump wavelength range provides valuable and quantitative information about the excited-state lifetimes, which reveals the excitation energy-dependent decay dynamics of electronically excited furfural and 5-methylfurfural. Further theoretical studies, like ab initio electronic structure calculations and high-level dynamics simulations, are strongly expected to provide a much deeper understanding of the ultraviolet photoinduced dynamics of these two molecular systems in the future.

■ ASSOCIATED CONTENT

Supporting Information

The Supporting Information is available free of charge at https://pubs.acs.org/doi/10.1021/acs.jpca.4c04503.

TRPES spectrum of 5-methylfurfural at a pump wavelength of 279.3 nm (DOCX)

■ AUTHOR INFORMATION

Corresponding Authors

Dongyuan Yang − *State Key Laboratory of Molecular Reaction Dynamics, Dalian Institute of Chemical Physics, Chinese Academy of Sciences, Dalian, Liaoning 116023, China*; orcid.org/0000-0001-9525-7885; Email: yangdy@dicp.ac.cn

Guorong Wu − *State Key Laboratory of Molecular Reaction Dynamics, Dalian Institute of Chemical Physics, Chinese Academy of Sciences, Dalian, Liaoning 116023, China*; orcid.org/0000-0002-0212-183X; Email: wugr@dicp.ac.cn

Authors

Wenping Wu − *State Key Laboratory of Molecular Reaction Dynamics, Dalian Institute of Chemical Physics, Chinese Academy of Sciences, Dalian, Liaoning 116023, China; University of Chinese Academy of Sciences, Beijing 100049, China*

Baihui Feng − *State Key Laboratory of Molecular Reaction Dynamics, Dalian Institute of Chemical Physics, Chinese Academy of Sciences, Dalian, Liaoning 116023, China; University of Chinese Academy of Sciences, Beijing 100049, China*

Yuhuan Tian − *State Key Laboratory of Molecular Reaction Dynamics, Dalian Institute of Chemical Physics, Chinese Academy of Sciences, Dalian, Liaoning 116023, China; University of Chinese Academy of Sciences, Beijing 100049, China*

Zhigang He − *State Key Laboratory of Molecular Reaction Dynamics, Dalian Institute of Chemical Physics, Chinese Academy of Sciences, Dalian, Liaoning 116023, China*

Xueming Yang − *State Key Laboratory of Molecular Reaction Dynamics, Dalian Institute of Chemical Physics, Chinese Academy of Sciences, Dalian, Liaoning 116023, China; Department of Chemistry, College of Science, Southern*

https://doi.org/10.1021/acs.jpca.4c04503
J. Phys. Chem. A XXXX, XXX, XXX−XXX

University of Science and Technology, Shenzhen 518055, China; orcid.org/0000-0001-6684-9187

Complete contact information is available at: https://pubs.acs.org/10.1021/acs.jpca.4c04503

Notes

The authors declare no competing financial interest.

■ ACKNOWLEDGMENTS

This experimental work was financially supported by the National Natural Science Foundation of China (grant nos. 22203095, 22103087, 22288201, and 21833003), the Key Technology Team of the Chinese Academy of Sciences (grant no. GJJSTD20220001), and the State Key Laboratory of Molecular Reaction Dynamics (grant no. SKLMRD-Z202406). We gratefully acknowledge the support and assistance provided by the Dalian Coherent Light Source (DCLS). We would also like to thank Xuegang Liu for very helpful discussions.

■ REFERENCES

(1) Marchetti, B.; Karsili, T. N. V.; Ashfold, M. N. R.; Domcke, W. A 'Bottom up', Ab Initio Computational Approach to Understanding Fundamental Photophysical Processes in Nitrogen Containing Heterocycles, DNA Bases and Base Pairs. *Phys. Chem. Chem. Phys.* **2016**, *18*, 20007−20027.

(2) Boldissar, S.; de Vries, M. S. How Nature Covers Its Bases. *Phys. Chem. Chem. Phys.* **2018**, *20*, 9701−9716.

(3) Gromov, E. V.; Trofimov, A. B.; Gatti, F.; Köppel, H. Theoretical Study of Photoinduced Ring-Opening in Furan. *J. Chem. Phys.* **2010**, *133*, 164309.

(4) Fuji, T.; Suzuki, Y. I.; Horio, T.; Suzuki, T.; Mitrić, R.; Werner, U.; Bonačić-Koutecký, V. Ultrafast Photodynamics of Furan. *J. Chem. Phys.* **2010**, *133*, 234303.

(5) Stenrup, M.; Larson, Å. A Computational Study of Radiationless Deactivation Mechanisms of Furan. *Chem. Phys.* **2011**, *379*, 6−12.

(6) Humeniuk, A.; Wohlgemuth, M.; Suzuki, T.; Mitrić, R. Time-Resolved Photoelectron Imaging Spectra from Non-Adiabatic Molecular Dynamics Simulations. *J. Chem. Phys.* **2013**, *139*, 134104.

(7) Spesyvtsev, R.; Horio, T.; Suzuki, Y. I.; Suzuki, T. Excited-State Dynamics of Furan Studied by Sub-20-fs Time-Resolved Photoelectron Imaging Using 159-nm Pulses. *J. Chem. Phys.* **2015**, *143*, No. 014302.

(8) Schalk, O.; Geng, T.; Hansson, T.; Thomas, R. D. The Ring-Opening Channel and the Influence of Rydberg States on the Excited State Dynamics of Furan and Its Derivatives. *J. Chem. Phys.* **2018**, *149*, No. 084303.

(9) Adachi, S.; Schatteburg, T.; Humeniuk, A.; Mitric, R.; Suzuki, T. Probing Ultrafast Dynamics During and after Passing through Conical Intersections. *Phys. Chem. Chem. Phys.* **2019**, *21*, 13902−13905.

(10) Filatov, M.; Lee, S.; Nakata, H.; Choi, C.-H. Signatures of Conical Intersection Dynamics in the Time-Resolved Photoelectron Spectrum of Furan: Theoretical Modeling with an Ensemble Density Functional Theory Method. *Int. J. Mol. Sci.* **2021**, *22*, 4276.

(11) Uenishi, R.; Boyer, A.; Karashima, S.; Humeniuk, A.; Suzuki, T. Signatures of Conical Intersections in Extreme Ultraviolet Photoelectron Spectra of Furan Measured with 15 fs Time Resolution. *J. Phys. Chem. Lett.* **2024**, *15*, 2222−2227.

(12) Oesterling, S.; Schalk, O.; Geng, T.; Thomas, R. D.; Hansson, T.; de Vivie-Riedle, R. Substituent Effects on the Relaxation Dynamics of Furan, Furfural and β-Furfural: A Combined Theoretical and Experimental Approach. *Phys. Chem. Chem. Phys.* **2017**, *19*, 2025−2035.

(13) Smith, A. R.; Meloni, G. Absolute Photoionization Cross Sections of Furanic Fuels: 2-Ethylfuran, 2-Acetylfuran and Furfural. *J. Mass Spectrom.* **2015**, *50*, 1206−1213.

(14) Jones, D. B.; Ali, E.; Nixon, K. L.; Limão-Vieira, P.; Hubin-Franskin, M.-J.; Delwiche, J.; Ning, C. G.; Colgan, J.; Murray, A. J.; Madison, D. H.; et al. Electron- and Photon-Impact Ionization of Furfural. *J. Chem. Phys.* **2015**, *143*, 184310.

(15) Ferreira da Silva, F.; Lange, E.; Limão-Vieira, P.; Jones, N. C.; Hoffmann, S. V.; Hubin-Franskin, M. J.; Delwiche, J.; Brunger, M. J.; Neves, R. F. C.; Lopes, M. C. A.; et al. Electronic Excitation of Furfural as Probed by High-Resolution Vacuum Ultraviolet Spectroscopy, Electron Energy Loss Spectroscopy, and Ab Initio Calculations. *J. Chem. Phys.* **2015**, *143*, 144308.

(16) Winfough, M.; Voronova, K.; Muller, G.; Laguisma, G.; Sztaray, B.; Bodi, A.; Meloni, G. Furfural: The Unimolecular Dissociative Photoionization Mechanism of the Simplest Furanic Aldehyde. *J. Phys. Chem. A* **2017**, *121*, 3401−3410.

(17) Bhattacherjee, A.; Schnorr, K.; Oesterling, S.; Yang, Z.; Xue, T.; de Vivie-Riedle, R.; Leone, S. R. Photoinduced Heterocyclic Ring Opening of Furfural: Distinct Open-Chain Product Identification by Ultrafast X-Ray Transient Absorption Spectroscopy. *J. Am. Chem. Soc.* **2018**, *140*, 12538−12544.

(18) He, Z.; Chen, Z.; Yang, D.; Dai, D.; Wu, G.; Yang, X. A New Khz Velocity Map Ion/Electron Imaging Spectrometer for Femtosecond Time-Resolved Molecular Reaction Dynamics Studies. *Chin. J. Chem. Phys.* **2017**, *30*, 247−252.

(19) Yang, D.; Chen, Z.; He, Z.; Wang, H.; Min, Y.; Yuan, K.; Dai, D.; Wu, G.; Yang, X. Ultrafast Excited-State Dynamics of 2,4-Dimethylpyrrole. *Phys. Chem. Chem. Phys.* **2017**, *19*, 29146−29152.

(20) Yang, D.; Min, Y.; Chen, Z.; He, Z.; Yuan, K.; Dai, D.; Yang, X.; Wu, G. Ultrafast Excited-State Dynamics of 2,5-Dimethylpyrrole. *Phys. Chem. Chem. Phys.* **2018**, *20*, 15015−15021.

(21) Yuan, W.; Yang, D.; Feng, B.; Min, Y.; Chen, Z.; Yu, S.; Wu, G.; Yang, X. Ultrafast Decay Dynamics of Electronically Excited 2-Ethylpyrrole. *Phys. Chem. Chem. Phys.* **2021**, *23*, 17625−17633.

(22) Feng, B.; Wu, W.; Yang, S.; He, Z.; Fang, B.; Yang, D.; Wu, G.; Yang, X. Insights into Ultrafast Decay Dynamics of Electronically Excited Pyridine-N-Oxide. *Phys. Chem. Chem. Phys.* **2024**, *26*, 8308−8317.

(23) Feng, B.; Wu, W.; He, Z.; Yang, D.; Wu, G.; Yang, X. Ultrafast Decay Dynamics of the $2^1\pi\pi^*$ Electronic State of N-Methyl-2-Pyridone. *J. Phys. Chem. A* **2024**, *128*, 3840−3847.

(24) Klapstein, D.; MacPherson, C. D.; O'Brien, R. T. The Photoelectron-Spectra and Electronic-Structure of 2-Carbonyl Furans. *Can. J. Chem.* **1990**, *68*, 747−754.

(25) Kotsina, N.; Townsend, D. Relative Detection Sensitivity in Ultrafast Spectroscopy: State Lifetime and Laser Pulse Duration Effects. *Phys. Chem. Chem. Phys.* **2017**, *19*, 29409−29417.

(26) Zwarich, R.; Rabinowitz, I. The Ultraviolet Vapor Absorption Spectrum of 2-Furaldehyde: Electronic Assignments and Vibrational Analysis. *J. Chem. Phys.* **1975**, *63*, 4565−4577.

(27) Gandini, A.; Hackett, P.; Back, R. The Photochemistry of 2-Furaldehyde Vapour. I. Photophysical Processes: Phosphorescence Excited in the π^* n Transition. *Can. J. Chem.* **1976**, *54*, 3089−3094.

(28) Min, Y.; Yuan, W.; Yang, D.; Dai, D.; Yu, S.; Wu, G.; Yang, X. Ultrafast Decay Dynamics of 2-Hydroxypyridine Excited to S_1 Electronic State. *Chin. J. Chem. Phys.* **2022**, *35*, 242−248.

(29) Yang, D.; Min, Y.; Chen, Z.; He, Z.; Chen, Z.; Yuan, K.; Dai, D.; Wu, G.; Yang, X. Ultrafast Dynamics of Water Molecules Excited to Electronic $\tilde{F}$ States: A Time-Resolved Photoelectron Spectroscopy Study. *Chin. J. Chem. Phys.* **2019**, *32*, 53−58.

(30) Yang, D.; Min, Y.; Feng, B.; Yang, X.; Wu, G. Vibrational-State Dependent Decay Dynamics of 2-Pyridone Excited to the S_1 Electronic State. *Phys. Chem. Chem. Phys.* **2022**, *24*, 22710−22715.

(31) Feng, B.; Yang, D.; He, Z.; Fang, B.; Wu, G.; Yang, X. Excitation Energy-Dependent Decay Dynamics of the S_1 State of N-Methyl-2-Pyridone. *J. Phys. Chem. A* **2023**, *127*, 10139−10146.

(32) El-Sayed, M. A. Spin-Orbit Coupling and the Radiationless Processes in Nitrogen Heterocyclics. *J. Chem. Phys.* **1963**, *38*, 2834−2838.

(33) Gandini, A.; Parsons, J. M.; Back, R. A. Photochemistry of 2-Furaldehyde Vapor. II. Photodecomposition: Direct Photolysis at

253.7 and 313 nm and Hg($^3P_1$)-Sensitized Decomposition. *Can. J. Chem.* **1976**, *54*, 3095−3101.

https://doi.org/10.1021/acs.jpca.4c04503
J. Phys. Chem. A XXXX, XXX, XXX−XXX